Design and Development of DC-Distributed System with Grid Connection for Residential Applications

T.-F. Wu, Y.-K. Chen*, G.-R. Yu and Y.-C. Chang

Elegant Power Application Research Center (EPARC)
National Chung Cheng University (CCU)
Ming-Hsiung, Chia-Yi, Taiwan, R.O.C.
E-mail: ieetfwu@ccu.edu.tw
Tel: 886-5-2428159; Fax: 886-5-2720862

*Department of Aeronautical Engineering
National Formosa University
Huwei Jen, Yunlin 632, Taiwan, R.O.C.
E-mail:ykchen@nfu.edu.tw
Tel: 886-5-6315543, Fax: 886-5-6312415

***Abstract*-- This paper presents design and development of a dc-distributed system with grid connection for residential applications. The system configuration is first described, including green power generator, energy storage element, dc appliance & equipment, and monitor & control center. For realizing the system, the kernel modules of bi-directional inverter, bi-directional charger/discharger, MPPT and dc appliance have been developed, and they are also introduced in this paper. A virtual house has been built in the CCU campus to demonstrate the system operation, from which test data and the critical issues being worth further study are presented.**

***Index Terms*-- dc-distribution system, grid connection**

I. INTRODUCTION

Global warming crisis and fossil energy depletion have been driving the eager need of developing renewable energy, which has been brought to many governments' attention worldwide. They have set the goal of increasing the usage of renewable energy to be higher than 20 % of their total power consumption by year 2020. For its unstable and unreliable properties, renewable energy is converted into dc and buffered with energy storage elements, and then it is inverted to ac and injected into utility grid. This approach can readily adapt to the existing electrical facility and expedite the applications of renewable energy. However, the existing high efficiency and/or compact size of appliance, equipment, 3C products, *etc.* are supplied by the dc which is converted from rectifying the ac source and with power actor correction. Thus, to use the renewable energy more efficiently and smartly, the dc electricity should be directly supplied to these loads. Such a supply scheme is far different from that of the conventional ac distribution and supply system. A configuration of the dc-distributed system with grid connection is shown in Fig.1, in which a bi-directional inverter is introduced to regulate the dc-grid voltage within a certain range.

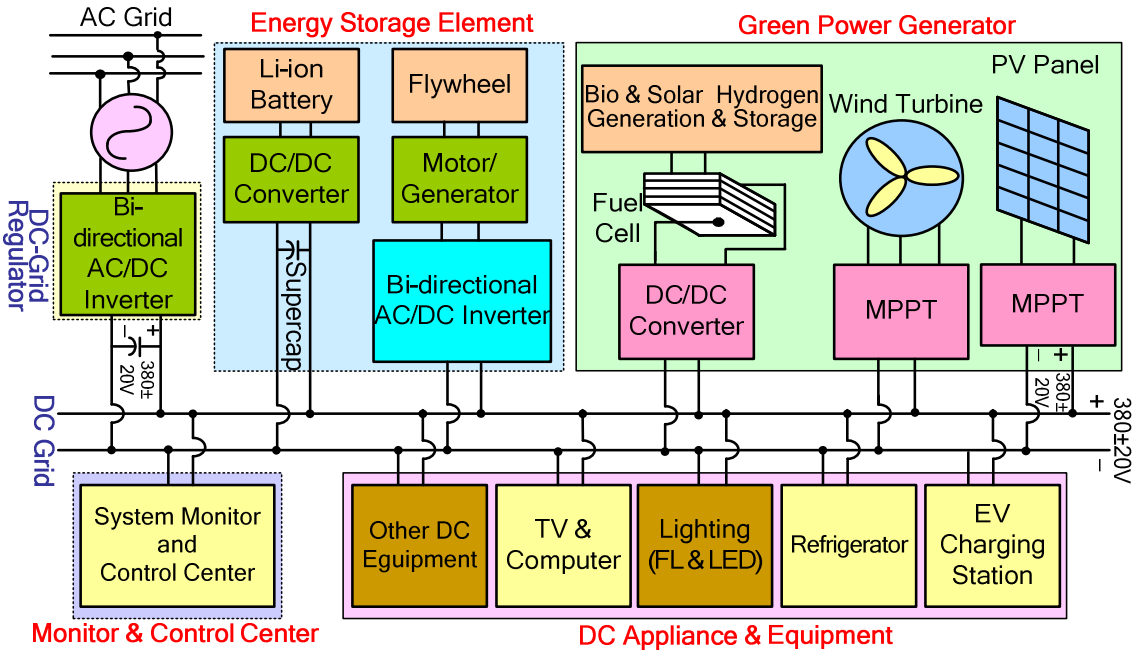

Fig. 1. Configuration of the dc-distributed system with grid connection

978-1-61284-957-7/11/$26.00 ©2011 IEEE

Recently, dc-distributed systems were applied to data centers [1]-[11], which can reduce power loss around 7 %, save space 33 %, reduce facility investment about 15% and increase reliability about 200 % [1]. Additionally, low voltage (24 V) ceiling-grid applications, especially for lighting, were also developed [12]-[16]. There are several research groups [17]-[32] having extended the high voltage (380 V) dc-distribution system to drive home appliances, of which the elegant power application research center (EPARC) has built a demonstration house for testing the overall system operation, as illustrated in Fig.1. In this paper, the system configuration including green power generator, energy storage element, dc appliance & equipment, and monitor & control center (MCC) will be introduced. Moreover, the developed kernel modules for realizing the system including bi-directional inverter (BDI), bi-directional charger/discharger (BDCD) and MPPT will be described. A linear dc-grid voltage regulation mechanism for reducing the frequency of operational mode changes will be also presented.

II. System Configuration and Operation

As shown in Fig.1, the system configuration includes five major blocks, green power generator, energy storage element, dc appliance & equipment, monitor & control center, and dc-grid regulator. The green power generator typically includes PV panels, wind turbines and fuel cells. The fuel cells provide base power for the loads. Maximum power point trackers (MPPT) are associated with PV panels and wind turbines to draw their maximum power, which is injected into the dc grid. The dc appliance & equipment are connected to the dc grid and supplied from the grid directly. If there is power shortage, the Li-ion battery will be first discharged to supply power for a short time interval and if the shortage lasts longer (*eg*. 2 min), the flywheel will start supplying power. In case, it lasts even longer (*eg*. 5 min), the BDI will buy power from the ac grid and it is operated in rectification mode with power factor correction (PFC) to regulate the dc-grid voltage within a certain range of 380 $\pm$ 20 V. Note that the battery discharger will be also responsible for dc-grid voltage regulation if the BDI is not in operation. On the other hand, if the BDI is in operation, the battery could be charged.

If there is power residue at the dc grid, the battery can be charged depending on its status of charge, the flywheel can be accelerated to store more energy, and/or the BDI can be operated in grid-connection mode to sell power and regulate the dc-grid voltage to 380 $\pm$ 20 V. The overall system operation will be monitored and controlled by the MCC, so that each module in the system has to communicate with the MCC based on CAN or ZigBee communication protocol. The MCC will command the modules when to operate and collect their operational status. However, under emergency conditions, such as over current, over voltage and over temperature, the modules will protect themselves without the command from the MCC, but the modules still have to inform the MCC of their current status.

III. Kernel Modules

The kernel modules in the dc-distributed system include BDI, BDCD, MPPT and dc appliance and product, and the design and development of each module is described as follows:

(I) Bi-directional Inverter

A single-phase bidirectional inverter is shown in Fig. 2, in which the inverter is a full-bridge topology associated with an *L-C* filter. The switches are realized with IGBTs and anti-parallel ultrafast diodes, and the inductor is constructed with an MPP core, in which the inductance varies from 4.3 mH to 630 μH when the current varies from zero to the peak value of 32 A. This inverter is with a 5 kW power rating, and with a predictive current control. The control laws of the inverter in grid-connection mode and rectification mode are shown as follows:

A. for grid connection (buck operation)

$$d_H(n+1)=\frac{\Delta i_L(n+1)\cdot L_s(i_L)}{V_{dc}(n)T_S}+\frac{V_s(n)}{V_{dc}(n)}, \quad (1)$$

where

$$\Delta i_L(n+1)=G_C\left(I_{ref}(n)-I_{fb}(n)\right)+\left(I_{ref}(n+1)-I_{ref}(n)\right),$$

T_s is the switching period, $L_s(i_L)$ is the inductance functioning of inductor current i_L , G_C is the error current compensator, and V_s is the ac source voltage.

B. for rectification mode (boost operation)

$$\overline{d}_H(n+1)=\overline{\left(\frac{\Delta i_L(n+1)\cdot L_s(i_L)}{v_{dc}(n)T_s}+\frac{v_s(n)}{v_{dc}(n)}\right)} \quad (2)$$

Or,

$$d_L(n+1)=1-\left(\frac{\Delta i_L(n+1)\cdot L_s(i_L)}{v_{dc}(n)T_s}+\frac{v_s(n)}{v_{dc}(n)}\right), \quad (3)$$

where d_H and d_L denote the duty ratios of the upper arm and the lower arm of *leg A*, respectively, and $\overline{d}_H = d_L$. In fact, boost operation is just the complementary operation of the buck. In (1) and (2), since inductance $L_s(i_L)$ is involved, the control laws can take into account the variation of inductance at every switching cycle.

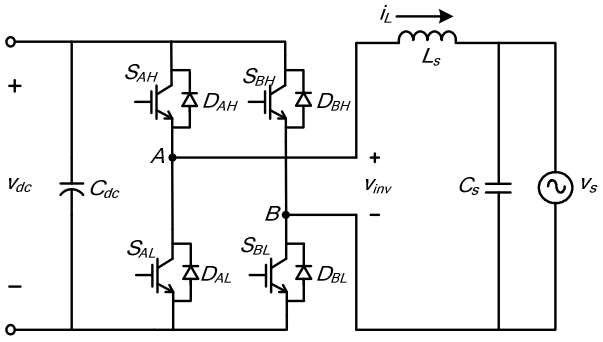

Fig. 2. Circuit diagram of a single-phase BDI.

A single-phase inverter is only good for low power applications. For high power applications, three-phase bi-directional inverters have been also developed, as shown in Fig. 3, in which the six-arm bridge type of topology is adopted and its connection to the ac source can be either a Δ-connection or a Y-connection. The control laws, which can take into account the inductance variation, for grid-connection mode and rectification modes are derived as follows:

A. for grid-connection mode

$$\begin{bmatrix} D_{RH} \\ D_{SL} \\ D_{TH} \end{bmatrix} = \begin{bmatrix} \dfrac{(L_R + L_S)\Delta i_{V(R)} + L_S \Delta i_{V(T)}}{v_{dc} T_s} \\ 0 \\ \dfrac{(L_T + L_S)\Delta i_{V(T)} + L_S \Delta i_{V(R)}}{v_{dc} T_s} \end{bmatrix} + \begin{bmatrix} \dfrac{v_{RS}}{v_{dc}} \\ 1 \\ -\dfrac{v_{ST}}{v_{dc}} \end{bmatrix}, \tag{4}$$

where D_{RH}, D_{SL} and D_{TH} are the duty ratios of switches S_{RH}, S_{SL} and S_{TH} denoted in Fig. 3, respectively, and the rest of them are set to zero. The control laws described by (4) is only good for the region of 0˚ ~ 60˚, as designated in Fig. 4. Analogously, the control laws for other regions can be also derived.

B. for rectification mode

Again, the inverter operated in grid-connection mode acts like a buck converter, while that in rectification mode is like a boost converter. Thus, the control laws for the rectification mode can be expressed as follows:

$$\overline{\begin{bmatrix} D_{RH} \\ D_{SL} \\ D_{TH} \end{bmatrix}} = \left\{ \begin{bmatrix} \dfrac{(L_R + L_S)\Delta i_{v(R)} + L_S \Delta i_{v(T)}}{v_{DC} T} \\ 0 \\ \dfrac{(L_T + L_S)\Delta i_{v(T)} + L_S \Delta i_{v(R)}}{v_{DC} T} \end{bmatrix} + \begin{bmatrix} \dfrac{v_{RS}}{v_{DC}} \\ 1 \\ -\dfrac{v_{ST}}{v_{DC}} \end{bmatrix} \right\} \tag{5}$$

Thus, equation (5) can be re-written as

$$\begin{bmatrix} \overline{D_{RH}} \\ \overline{D_{SL}} \\ \overline{D_{TH}} \end{bmatrix} = \begin{bmatrix} 1 \\ 1 \\ 1 \end{bmatrix} - \left(\begin{bmatrix} \dfrac{(L_R + L_S)\Delta i_{v(R)} + L_S \Delta i_{v(T)}}{v_{DC} T} \\ 0 \\ \dfrac{(L_T + L_S)\Delta i_{v(T)} + L_S \Delta i_{v(R)}}{v_{DC} T} \end{bmatrix} + \begin{bmatrix} \dfrac{v_{RS}}{v_{DC}} \\ 1 \\ -\dfrac{v_{ST}}{v_{DC}} \end{bmatrix} \right). \tag{6}$$

Or,

$$\begin{bmatrix} D_{RL} \\ D_{SH} \\ D_{TL} \end{bmatrix} = -\begin{bmatrix} \dfrac{(L_R + L_S)\Delta i_{v(R)} + L_S \Delta i_{v(T)}}{v_{DC} T} \\ 0 \\ \dfrac{(L_T + L_S)\Delta i_{v(T)} + L_S \Delta i_{v(R)}}{v_{DC} T} \end{bmatrix} + \begin{bmatrix} 1 - \dfrac{v_{RS}}{v_{DC}} \\ 0 \\ 1 + \dfrac{v_{ST}}{v_{DC}} \end{bmatrix}. \tag{7}$$

In the above equations, $D_{\bullet H}$ and $D_{\bullet L}$ denote the duty ratios of the upper arm and the lower arm, respectively, and $\bar{D}_{\bullet H} = D_{\bullet L}$. Note that again they are only good for region 0˚ ~ 60˚. For other regions, the control laws can be also derived by following the same procedure and based on those derived in grid-connection mode.

The three-phase BDI can function as a dc-grid regulator or a driver for the flywheel to draw or store energy. Moreover, for reducing cost, the BDCD can be designed with low power rating, and the BDI is operated as a charger/discharger with high power rating for dc UPS applications, as illustrated in Fig. 5.

Recently, there was a request of providing reactive power for the ac grid from the inverter with a power rating higher than 20 kVA. In fact, this is equivalent to operating the inverter both in grid-connection and rectification modes within a line cycle. The proposed BDI can meet this request by simply changing the operational modes according to the desired power factor.

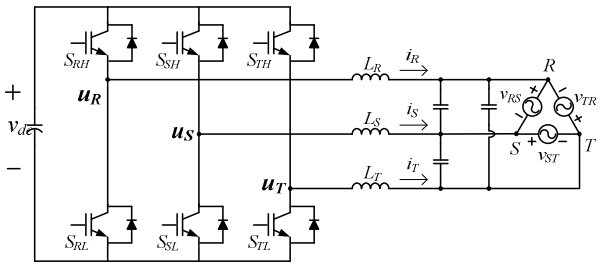

Fig. 3. Circuit diagram of a three-phase BDI.

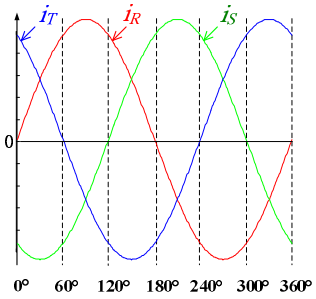

Fig. 4. Six regions in one line period divided according to the zero-crossing points of line currents i_R, i_S and i_T.

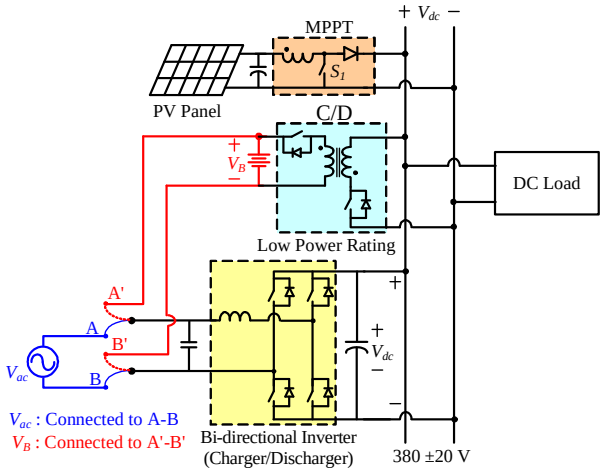

Fig. 5. Circuit diagram of the BDI acting like a charger/discharger.

(II) Bi-directional Charger / Discharger

The BDCD is designed for charging/discharging Li-ion battery. Its circuit configuration is shown in Fig. 6 for high power applications. The low voltage side is a 48 V battery, while the high voltage side is the dc grid. A flyback snubber is introduced to absorb the current difference between those of the primary inductor and the leakage inductance. In addition, the flyback snubber can be used to pre-charge the high side bulky capacitor under

UPS mode, which can prevent the switches at the low side from inrush current.

For Charging mode, the BDCD acts like a step-down converter, in which switches $M_5 \sim M_8$ are operated with phase-shift manner to achieve ZVS turn on, and $M_1 \sim M_4$ are operated with synchronous rectification to reduce conduction loss. Leakage inductance L_{lh} and L_{ll} can help to limit the reverse recovery current from the body diodes of $M_1 \sim M_4$.

For discharging mode, the BDCD acts like a step-up boost converter, in which switches $M_1 \sim M_4$ are all turned on to magnetize primary inductor L_m, and $M_5 \sim M_8$ act like a full-bridge rectifier and with synchronous rectification. When switches $M_1 \sim M_4$ are operated in diagonal position, the energy stored in L_m will be transferred to the high side. However, at the transition, there exists current difference between i_L and i_p, resulting in high voltage spike. Thus, capacitor C_c and diode d_c are introduced to absorb this current difference and clamp the rail voltage. The energy stored in C_c is then discharged by the flyback snubber and transferred to the high side. This flyback snubber will process about 2 % of the full power rating (1.5 kW), and clamp the capacitor C_c voltage to a desired value around $V_{HV} \cdot N_p / N_s$.

The BDCD can be also adopted to boost the fuel cell output voltage and connect to the dc grid when electrical isolation is required.

(III) Maximum Power Point Tracker

In this system, the MPPT for PV panels is realized by a boost converter associated with flyback and passive snubbers, as shown in Fig. 7, in which diode D_1 and capacitor C_s provide a path for absorbing the current difference between inductor currents i_{Lm} and i_{Ls}. The flyback snubber will then transfer the energy stored in C_s to capacitor C_b which can help to reduce turn-off loss and voltage stress of switch S_m. Moreover, with this configuration, the discharging current of capacitor C_b will not circulate through main switch S_m. Thus, the snubbers can achieve near ZVS turn-on and near ZCS turn-off for S_m and can reduce its voltage and current stress, achieving the highest efficiency of 98.5 %.

The MPPT for the wind turbine will have two choices. One is to track the rectified maximum power point, and the converter shown in Fig. 7 still can be used. The other is to adopt the BDI shown in Fig. 3, which can track the maximum power point of the wind turbine and fulfill power factor correction to achieve high power factor.

For simplifying control complexity and reducing the sensitivity to sampling noise, the perturb & observe scheme is implemented in a micro-controller for tracking the maximum power point.

(IV) DC-Appliance and Product

The dc appliances and products were modified from the existing ac ones. Typically, high efficiency products, such as electronic ballast, variable speed air conditioner, refrigerator, washing machine, fan and computer, are supplied with dc source which is converted from ac source with power factor correction. Thus, the dc products can be simply modified by just removing the power factor corrector located in front of the power processor and rerouting the protection wire and circuitry. In this study, we have modified the following products: air conditioner, TV, refrigerator, washing machine, oven, fan, computer, LED driver and electronic ballast. These are all done by the manufacturers and the researchers in EPARC. The input bulky capacitors are removed and combined with the dc grid capacitors which are packed in a box. For control and monitoring, each dc product is equipped with a CAN or ZigBee communication port. Additionally, the products are classified into two types. One is a regular type, the other is an emergency type. When ac source is available, these two types of dc products can be supplied from the dc grid. While, if the ac is in black out and the power available in dc grid is only from the green source and battery, only are the emergency type of dc products can operate. This will help to reduce inrush current when the ac source comes back to supply power again.

As mentioned previously, all of the input bulky capacitors are removed from the dc products. To reduce transient voltage fluctuation, each dc product is designed with soft start and soft shutdown. Without the bulky capacitors, when the power plug is unplugged from the socket, the input EMI filter capacitor can be discharged in a short time interval. Thus, even though there is no input blocking diode, as illustrated in Fig. 8, electric shock can be avoided readily, and power loss to the diode can be saved.

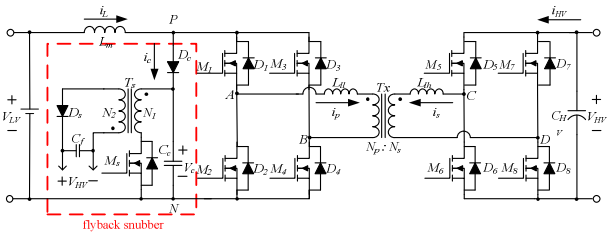

Fig. 6. Circuit configuration of a bi-directional charger/discharger with isolation.

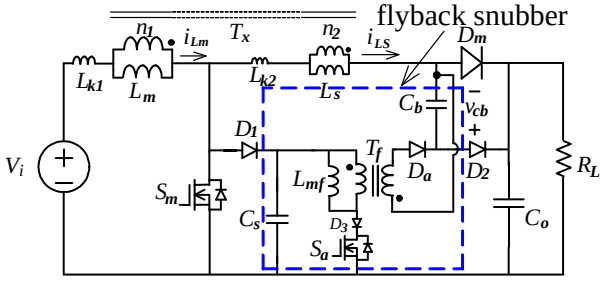

Fig. 7. Boost converter with flyback and passive snubbers functioning as an MPPT for PV panels.

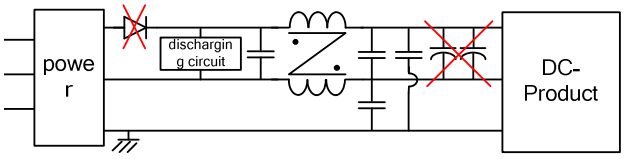

Fig. 8. Conceptual illustration of an input section of the dc products.

(V) DC-Grid Regulation

To reduce the dc-grid capacitance and the frequency of mode changes, a linear dc-grid voltage regulation algorithm is implemented, as illustrated in Fig. 9. If the BDI sells a higher power level which means less number of dc products in operation, the dc-grid voltage is regulated to a higher value. The reason is that if there are dc products turned on suddenly, the voltage will not drop below 380 V right away and it will not charge the operation modes from grid connection to rectification. On the other hand, when the BDI buys a higher power level, the dc grid is regulated to a lower voltage level, reducing mode-change frequency.

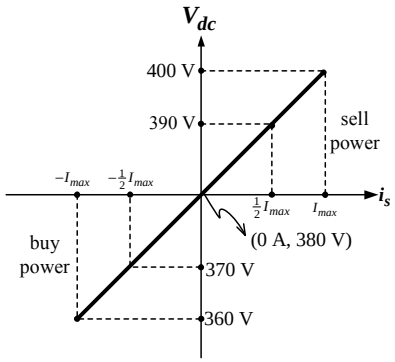

Fig. 9. Plot of V_{dc} vs. i_s for illustrating a linear dc-grid voltage regulation algorithm.

IV. Demo. House and Measured Results

For the demo. house, as shown in Fig. 10, the manufacturers from SAMPO, TECO, Eulife, Jamicon, Fego, *etc*., have helped to modify their ac products to the dc ones. Additionally, a set of dc power plug and socket connected with the dc products, which can eliminate arking, has been supported by Fujitsu. We have collected the operational data from the system, which shows that the dc products supplied from the dc grid can save 8.5% of power consumption over their ac counterparts. The measured voltage and current waveforms from the kernel modules are shown in Figs. 11~14, which have confirmed the discussions.

An infrastructure of the dc-distributed system with grid connection for residential applications has been proposed. However, there are still a lot of details needed to be figured out further, as listed in the following:

1) short-circuit protection at both dc grid and product sides,
2) EMI filter and capacitor discharging circuit for dc products,
3) pre-charge and protection for the bulky capacitor pack,
4) communication protocol among the kernel modules,
5) features of dc products, and
6) safety codes for the system.

Fig. 10. Photographs of the dc products in the EPARC demo. House.

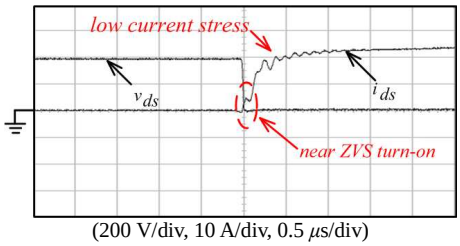

(200 V/div, 10 A/div, 0.5 μs/div)

(a)

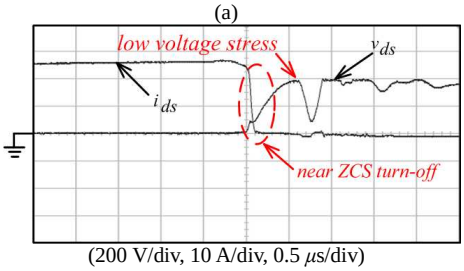

(200 V/div, 10 A/div, 0.5 μs/div)

(b)

Fig. 11. Measured waveforms from the proposed boost + flyback converter shown in Fig. 7.

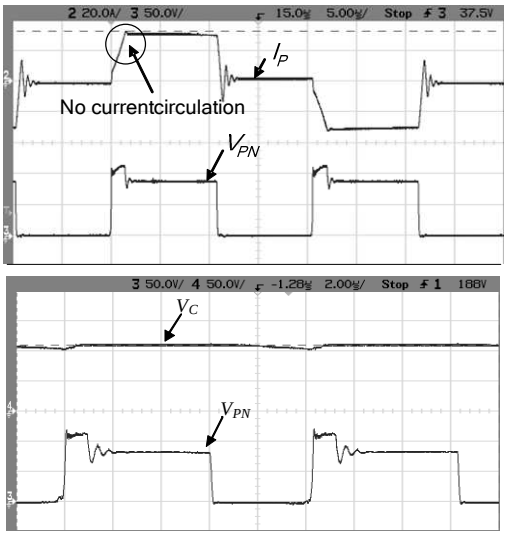

Fig. 12. Measured waveforms from the BDCD illustrating clamped rail voltage and no current circulation through switches M_1 ~ M_4 in Fig. 6.

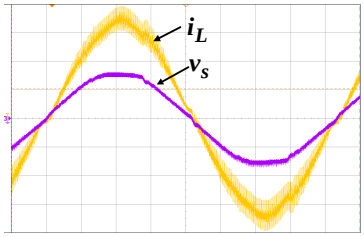

(i_L: 10.0A/div, v_s : 200 V/div, 2ms/div)

(a)

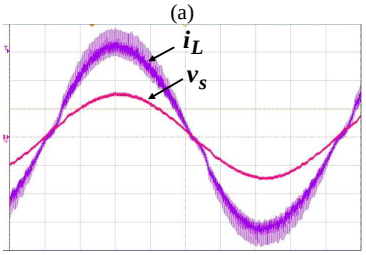

(i_L: 10.0A/div, v_s : 200 V/div, 2ms/div)

(b)

Fig. 13. Measured waveforms from the 1ϕ BDI in (a) grid-connection mode, and (b) rectification mode with 5 kW power rating.

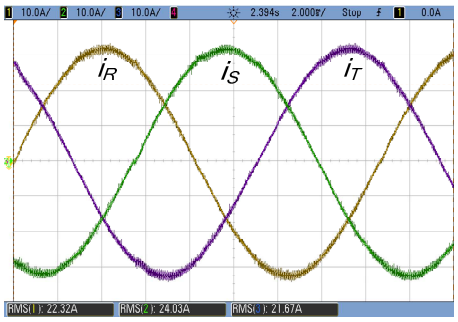

(i_R, i_S and i_T: 10 A/div; time: 2ms/div)

(a)

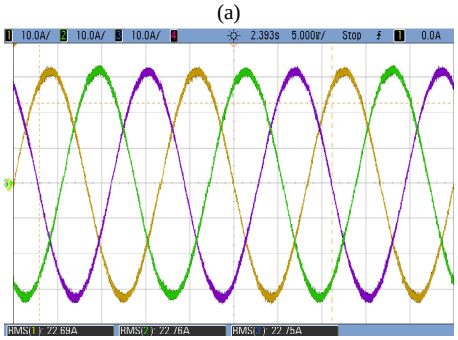

(i_R, i_S and i_T: 10 A/div; time: 2ms/div)

(b)

Fig. 14. Measured waveforms for the 3ϕ BDI in (a) grid-connection mode, and (b) rectification mode with 10 kW power rating.

V. CONCLUSIONS

A dc-distributed system with grid connection for residential applications has been introduced in this paper. Design and development of the kernel modules, including bi-directional inverter, bi-directional charger / discharger, MPPT for PV panels and wind turbines, and dc appliance and product has been also presented. Additionally, a linear dc-grid voltage regulation scheme has been proposed to reduce mode-change frequency. Measured results from the developed kernel modules have verified the discussion. In the paper, several issues needed to be further studied have been also pointed out.

ACKNOWLEDGEMENT

The authors would like to thank the National Science Council, Taiwan, ROC, for the funding with the project number:NSC99-3113-P-194-001

REFERENCES

[1] Experience in Developing and Promoting 400Vdc Datacenter Power, *Tomm V. Aldridge, Director, Energy Systems Research Lab, Intel Corporate Technology Group, Green Building Power Forum, Jun. 2009.*

[2] Maximizing Overall Energy Efficiency in Data Centres, *Stefan Lidstrom, CTO, Netpower Labs AB, Green Building Power Forum, Jun. 2009.*

[3] Renewable Energy & Data Centers, *Jack Pouchet, Director Energy Initiatives, Emerson Network Power., Green Building Power Forum, Jun. 2009.*

[4] Development of Higher Voltage Direct Current Power Feeding System in Data Centers, *Kaoru Asakura, NTT Energy/Environment, Green Building Power Forum, Dec. 2010.*

[5] Specifications for 400V DC Power Supplies and Facility

Equipment, *Dennis Symanski, Sr. Program Manager, Electric Power Research Institute, Keiichi Hirose, NTT Facilities, and Brian Fortenberry, Program Manager, Electric Power Research Institute, Green Building Power Forum, Jan. 2010.*

[6] Development of a DC Power Inlet Connector for 400Vdc IT Equipment, *Brian Davies, Director of Engineering, Anderson Power Products, Inc. Green Building Power Forum, Jan. 2010.*

[7] Development of Socket-outlet Bar and Power Plug for 400V Direct Current Feeding System, *Takashi Yuba, R&D Manager, Fujitsu Components Ltd. Green Building Power Forum, Jan. 2010.*

[8] Power Inlet Connector for 380V DC Data Center, *Brain Davies, Anderson Power Products, Green Building Power Forum, Dec. 2010.*

[9] Intel Lab's New Mexico Energy System Research Center 380V DC Microgrid Testbed, *Guy Allee, Intel Labs, Green Building Power Forum, Dec. 2010.*

[10] International Standardization of DC Power, *Keiichi Hirose, NTT Facilities, Green Building Power Forum, Dec. 2010.*

[11] R. Simanjorang, H. Yamaguchi, H. Ohashi, K. Nakao, T. Ninomiya, S. Abe, M. Kaga, A. Fukui *"High-Efficiency High-Power dc-dc Converter for Energy and Space Saving of Power-Supply System in a Data Center," APEC'11 , 2011, pp. 600-605.*

[12] Direct Powered DC Lighting Technologies, Jonathan Busch, Commerical Engineer, *Osram Sylvania Inc. Green Building Power Forum, Jun. 2009.*

[13] An Exploration of the Technical and Economic Feasibility of a Low-Powered DC Voltage Mains Power Supply in the Domestic Arena, *Moshe C.* Kinn, University of Manchester, *Green Building Power Forum, Jun. 2009.*

[14] DC Input Dimmable Fluorescent Ballast, *Tom Ribarich, Vice President, International Rectifier, Green Building Power Forum, Jun. 2009.*

[15] Low-Voltage DC Interconnection, *John Akins, Director of Business Development, Tyco Electronics, Green Building Power Forum, Jan. 2010.*

[16] Advantages of Low-Voltage DC Power in Commercial Building Interiors, *Bruce Graham, President, Projects/Design & Construction division of Johnson Control, Green Building Power Forum, Jan. 2010.*

[17] DC Distribution and the Home of the Future, *Brain Fortenbery, Program Manager, Electric Power Research Institute, Green Building Power Forum, Jun. 2009.*

[18] DC Nanogrid for Sustainable Building, Dushan Boroyevich, *Fred Wang, Fred C. Lee, lgor Cvetkovi ć, Dong Jiang, Timothy Thacker, Dong Dong, Center for Power Electronics Systems, The Bradley Department of Electrical and Computer Engineering, Virginia Polytechnic Institute and State University, Green Building Power Forum, Jun. 2009.*

[19] Optimizing Efficiency and Reliability of DC Branch Circuits in Buildings, *Don Mulvey, Executive VP, Roal Electronics USASession 2 – Emerge Alliance Activities, Green Building Power Forum, Jan. 2010.*

[20] Design, Implementation and Operation of DC Micro Grid and DC Appliances, *Tsai Fu Wu, Professor EE, National Chung Cheng University, Green Building Power Forum, Jan. 2010.*

[21] Buildings with low energy consumption in Germany, *Ulrich Boeke, Philips, Green Building Power Forum, Jan. 2010.*

[22] Green Energy DC-Distribution System with Grid Connection, *Tsai Fu Wu, National Chung Cheng University, Green Building Power Forum, Dec. 2010.*

[23] Modeling and Analysis of DC Power Distribution Systems for Residential and Commercial Buildings, *Gab-Su Seo, Seoul National University, Green Building Power Forum, Dec. 2010.*

[24] DC Power Systems for Sustainable Buildings, *Igor Cvetkovic, Virginia Polytechnic University, Green Building Power Forum, Dec. 2010.*

[25] Concept of Fukuoka Smart House - Achievement of Hybrid System in Renewable Energy and Grid, *Yoshimichi Nakamura, Smart Energy Laboratory, Green Building Power Forum, Dec. 2010.*

[26] A Modification Guideline for Electrical Appliances Compatible with DC Distribution Systems, *Kyusik Choi, Seoul National University, Korea, Green Building Power Forum, Dec. 2010.*

[27] H. Kakigano, A. Nishino, Y. Miura and T. Ise, *"Distribution Voltage Control for DC Microgrid by Converters of Energy Storages Considering the Stored Energy," ECCE'10, 2010, pp. 2851-2856.*

[28] L. Zhang, T. Wu, Y. Xing, K. Sun, and J. M. Gurrero *"Power Control of DC Microgrid Using DC Bus Signaling," APEC'11 , 2011, pp. 1926-1932.*

[29] T.-F. Wu, K.-H. Sun, C.-L. Kuo, and G.-R. Yu, *"Current Distortion Improvement and DC-link Voltage Regulation for Bi-directional Inverter in DC-Microgrid Applications," APEC'11 , 2011, pp. 1582-1587.*

[30] D. Dong, F. Luo, W. Zhang, D. Boroyevich, P. Mattavelli, I. Cvetkovic, L. Jiang, and P. Kong, *"Passive Filter Topology Study of Single-phase ac-dc Converters for DC Nanogrid Applications," APEC'11 , 2011, pp. 287-294.*

[31] A. Stupar, T. Friedli, J. Miniböck, M. Schweizer, and J. W. Kolar, *"Towards a 99% Efficient Three-Phase Buck-Type PFC Rectifier for 400 V DC Distribution Systems," APEC'11 , 2011, pp. 505-512.*

[32] I. Cvetkovic, D. Boroyevich, P. Mattavelli, F. C. Lee, and D. Dong, *"Non-linear, Hybrid Terminal Behavioral Modeling of a DC-based Nanogrid System," APEC'11 , 2011, pp. 1251-1258.*